

Configuration space Faddeev calculations. IV. Trinucleon charge density

J. L. Friar and B. F. Gibson

Theoretical Division, Los Alamos National Laboratory, Los Alamos, New Mexico 87545

E. L. Tomusiak

*Los Alamos National Laboratory and Department of Physics,
University of Saskatchewan, Saskatoon, Saskatchewan S7N 0W0, Canada*

G. L. Payne

*Los Alamos National Laboratory and Department of Physics and Astronomy,
University of Iowa, Iowa City, Iowa 52242*

(Received 23 March 1981)

The charge densities of ${}^3\text{H}$ and ${}^3\text{He}$ are computed for several potential models. These densities are further broken down into isospin components and into components from the S , S' , and D states. Wave functions for these states are plotted in order to illustrate the structure seen in the densities. Inclusion of nucleon finite size eliminates the fine structure seen in the point nucleon cases. Form factors corresponding to those densities are also calculated. The inclusion of a Coulomb interaction between the two protons in ${}^3\text{He}$ is seen to produce a small but nonnegligible change in the density. The theoretical ${}^3\text{He}$ densities for the Reid soft core model are compared to the "experimental" one obtained by fitting the experimental form factor data after having approximately removed the effect of nucleon finite size. The central depression seen in the experimental density is not present in the theoretical ones, and we speculate on this and other discrepancies.

[NUCLEAR STRUCTURE Trinucleon system, charge density, wave function components, Coulomb interaction.]

I. INTRODUCTION

Approximately 15 years ago, the first experiments¹ were performed to measure the form factors of the ground states of the trinucleon system, ${}^3\text{He}$ and ${}^3\text{H}$. These electron scattering measurements were limited to a modest range of momentum transfer. Subsequent measurements² of the ${}^3\text{He}$ form factor were extended to very high momentum transfer,³⁻⁶ so that a reasonably plausible inversion of the Fourier transform could be made in order to obtain $\rho(r)$, the ${}^3\text{He}$ charge density. This density contains a substantial central depression,⁷ and provides a serious challenge to theorists, since no consensus exists concerning its origin. Insufficient data exist for the inversion to be performed for ${}^3\text{H}$.

The lack of ${}^3\text{H}$ data has focused theoretical attention on ${}^3\text{He}$, particularly on the charge form factor, to the near exclusion of ${}^3\text{H}$. The presence of a central depression in the density is concomitant with

the existence of a very strong secondary maximum in the form factor, which has proven difficult to reproduce. The sum rule which follows from the Fourier transform inversion theorem^{8,9}

$$\rho(0) = \frac{1}{2\pi^2} \int_0^\infty F(q^2)q^2 dq$$

clearly relates the high- q part of the form factor F to $\rho(0)$, and the existence of a strong *negative* secondary maximum after the first diffraction minimum depresses $\rho(0)$. Although many have calculated the form factors¹⁰⁻¹⁷ of ${}^3\text{He}$ and ${}^3\text{H}$, few have calculated the ${}^3\text{He}$ density^{7,18-20} and fewer still that of the triton.¹⁸⁻²⁰ To the best of our knowledge, no one has calculated separate isospin components.

It is our belief that the densities are easier to interpret intuitively and physically. In addition, previous calculations of the ${}^3\text{He}$ density were not always consistent even for the same potential model.²¹ For these reasons we present in this paper our results for

both of the trinucleon charge densities calculated from wave functions obtained by solving the nonrelativistic Faddeev-Noyes equations¹³ in configuration space for the Reid soft core (RSC) model in the 5-channel (1S_0 , 3S_1 - 3D_1) approximation. We have fully described our techniques elsewhere^{22,23} and will not do so here. The structure of the charge densities will be compared and contrasted and later analyzed in terms of wave function components.²⁴ In addition, these densities will be separated into isospin components and analyzed. The effect of including the Coulomb interaction between protons in ^3He is shown to be small, as intuition suggests, but not negligible. Form factors are also calculated, and the effect of folding the point trinucleon densities with the individual nucleon densities is shown to eliminate the fine structure seen in the former when a tensor force is included in the nucleon-nucleon potential. Finally, we argue for comparable ^3H experiments, in order to help unravel the mysteries of the trinucleon structure, and speculate on the possible origins of various discrepancies.

II. CHARGE DENSITIES

There are a variety of ways to decompose the trinucleon form factors. Our choice uses an obvious, but unconventional notation. The point nucleon density matrix elements have the form

$$\rho \begin{pmatrix} p \\ n \end{pmatrix} (r) = \left\langle \Psi \left| \sum_i \left[\frac{1 \pm \tau_3(i)}{2} \right] \delta^3(\vec{r} - \vec{x}'_i) \right| \Psi \right\rangle, \quad (1)$$

where \vec{x}'_i is the coordinate of nucleon i relative to the nuclear center of mass. The form factors corresponding to ρ_p and ρ_n are denoted F_p and F_n . Introduction of nucleon finite size (i.e., charge distributions) is accomplished by replacing the δ^3 function by $g_E(|\vec{r} - \vec{x}'_i|)$, the Fourier transform of the experimentally observed nucleon form factor, $G_E(q^2)$:

$$G_E(q^2) = \int d^3r e^{i\vec{q}\cdot\vec{r}} g_E(r) \quad (2a)$$

and

$$g_E(r) = \frac{1}{(2\pi)^3} \int d^3q e^{i\vec{q}\cdot\vec{r}} G_E(q^2). \quad (2b)$$

Since we use the convention $G_E(0) \equiv 1$ for the proton, this translates into $\int d^3r g_E(r) = 1$. Denoting folded densities by an overscore, we deduce the ob-

vious relationships²⁵

$$\overline{\rho}(r) = \int d^3r' g_E(|\vec{r} - \vec{r}'|) \rho(r') \quad (3a)$$

$$= \frac{1}{2r} \int dr' r' [h(r+r') - h(|r-r'|)] \rho(r'), \quad (3b)$$

where

$$h(z) = 4\pi \int^z dy y g_E(y). \quad (3c)$$

Since the trinucleon system has Z protons and N neutrons we have the obvious constraints

$$\int d^3r \rho \begin{pmatrix} p \\ n \end{pmatrix} (r) = \begin{pmatrix} Z \\ N \end{pmatrix}. \quad (4)$$

Because it is convenient to compare densities which are normalized to 1 (or 0 in some cases) we define²⁶ our form factors by

$$\begin{aligned} 2\overline{F}_{\text{He}} &= G_E^p(2F_s + F_v) + G_E^n(F_s - F_v) \\ &= F_s(2G_E^p + G_E^n) + F_v(G_E^p - G_E^n) \\ &= 2[F_s G_E^s + (F_v G_E^v - F_s G_E^n)/2] \\ &\equiv 2(\overline{F}_s + \overline{F}_v/2), \end{aligned} \quad (5a)$$

$$\begin{aligned} \overline{F}_{\text{H}} &= G_E^p(F_s - F_v) + G_E^n(2F_s + F_v) \\ &= F_s(G_E^p + 2G_E^n) - F_v(G_E^p - G_E^n) \\ &= F_s G_E^s - (F_v G_E^v - F_s G_E^n) \\ &\equiv \overline{F}_s - \overline{F}_v, \end{aligned} \quad (5b)$$

where $G_E^p(0) = 1$, $G_E^n(0) = 0$, $G_E^s \equiv G_E^p + G_E^n$, $G_E^v \equiv G_E^p - G_E^n$,

$$F_p \equiv 2F_s + F_v, \quad (5c)$$

and

$$F_n \equiv F_s - F_v. \quad (5d)$$

The corresponding densities are given by

$$\rho_{\text{He}} = \rho_s + \rho_v/2 \quad (6a)$$

and

$$\rho_{\text{H}} = \rho_s - \rho_v. \quad (6b)$$

The introduction of finite size is done in the obvious way by folding g_E^s with ρ_s (yielding $\overline{\rho}_s$), and the difference of folding g_E^v with ρ_v and folding ρ_s with g_E^n , yielding $\overline{\rho}_v$. Thus ρ_s is the isoscalar density, while ρ_v is not the true isovector density, but rather the *difference* density. The distinction is necessary

only because of the factor of 2 in Eqs. (5a) and (5c), and because the actual isovector density contains a component proportional to ρ_s . Clearly, we also have

$$\rho_s = \frac{2\rho_{\text{He}} + \rho_{\text{H}}}{3} \quad (7a)$$

and

$$\rho_v = \frac{2(\rho_{\text{He}} - \rho_{\text{H}})}{3}. \quad (7b)$$

We have chosen to use the nucleon form factor fits (8.2) of Höhler *et al.*²⁷ because of their attention to detail in handling the experimental errors and because they include both proton and neutron data. In addition, because they fit the form factors using a sum of poles and dipoles, the nucleon charge densities $g_E(r)$, are written as a sum of Yukawa functions and exponentials; in such cases the integral (3c) can be performed analytically, which greatly facilitates computation.

III. RESULTS AND CALCULATIONS

Figure 1 depicts the various point densities (no nucleon finite size) for the Malfliet-Tjon (MT)

I–III potential,²⁸ a purely *S*-wave force with short-range repulsion which generates a binding energy and radius close to the experimental values.²² The densities are a smooth function of the radius variable r . The form of the vector density is dictated by three considerations: the fact that $\int d^3r \rho_v(r) \equiv 0$; the relative weakness of the force between two protons compared to the neutron-proton force; and the signs in Eq. (6). In ${}^3\text{He}$ the protons feel a weaker force than does the neutron, and this causes the protons to lie further from the nuclear center of mass (on the average) than does the neutron, which generates a preferred isosceles configuration rather than simply an equilateral one. The opposite is true in ${}^3\text{H}$, with the proton lying closer. Therefore, the charge radius of ${}^3\text{He}$ must be greater than ${}^3\text{H}$ and ρ_v has a positive mean-square radius. Consequently, ρ_v must be positive at large r and it must be negative at small distances in order to conserve charge.

The effect of adding a tensor force is illustrated in Figs. 2 and 3, which were calculated using the Reid soft core model in the 3-channel and 5-channel approximations, the former being an incomplete treatment of the tensor force in the ${}^1S_0, {}^3S_1 - {}^3D_1$ partial waves. The primary difference is a depressed scalar

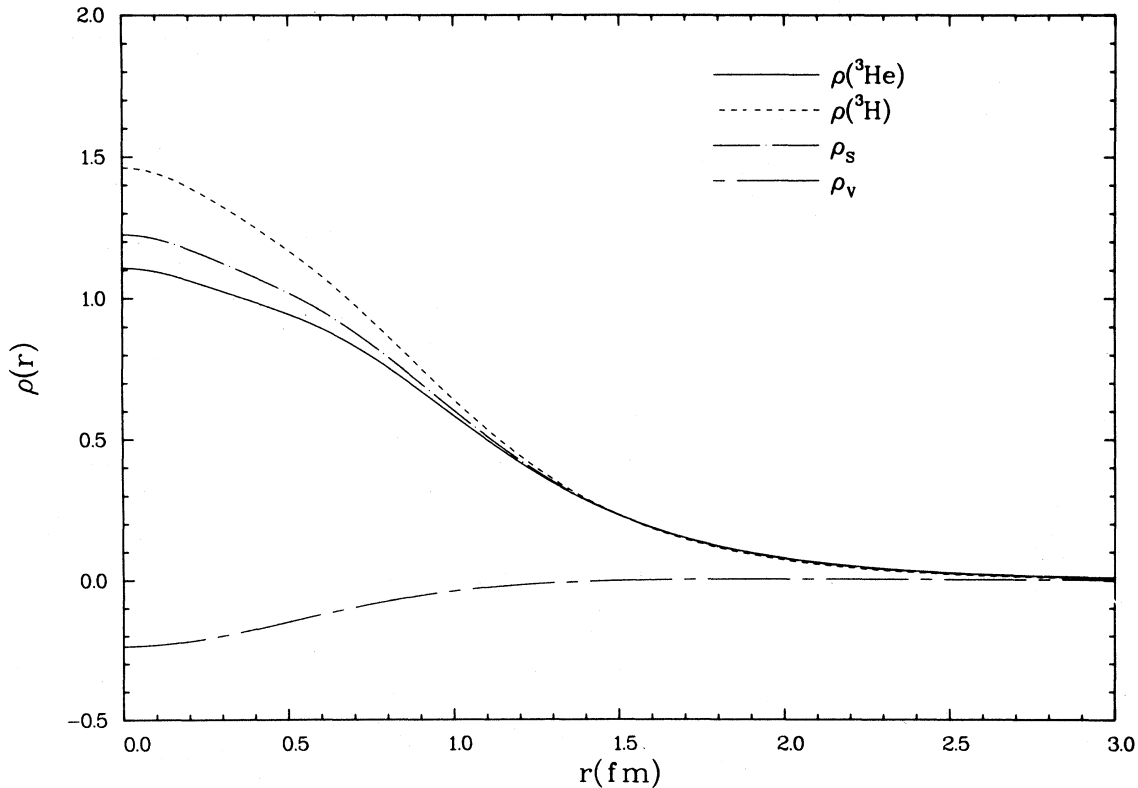


FIG 1. Various point nucleon charge density components of the trinucleon system calculated using the Malfliet-Tjon I–III (MT I–III) *S*-wave potential model.

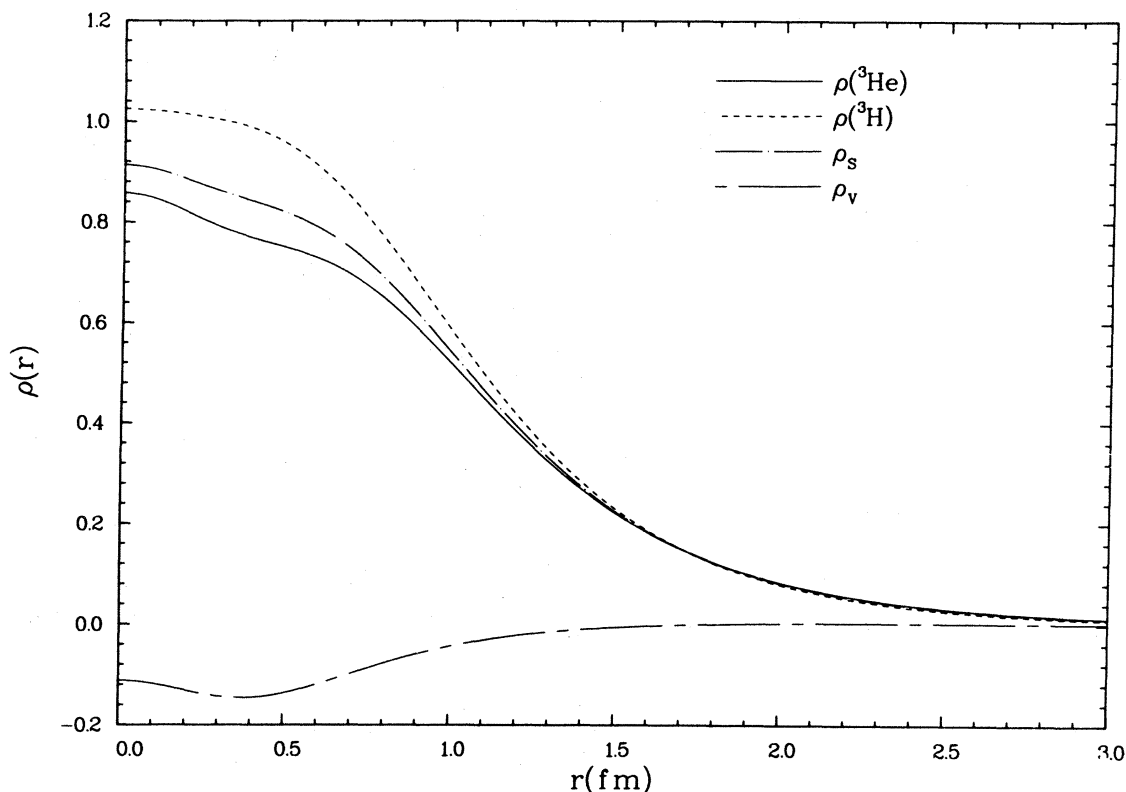


FIG. 2. Various point nucleon charge density components of the trinucleon system calculated using the 3-channel approximation and the Reid soft core potential model.

density ρ_s and an enhanced value of ρ_v at the origin for the latter case, which depresses ρ_{He} slightly and ρ_{H} significantly compared to the former case. The reason for the fine structure in ρ_v , ρ_{He} , and ρ_{H} at small values of r will be discussed shortly.

The effect of folding in the nucleon charge densities is illustrated in Fig. 4. All of the fine structure visible in Fig. 3 has been ironed out. With the exception of a scale change, all of the folded densities that we have calculated look alike. The reason is obvious: nucleons have a size of nearly 1 fm, and folding smears out the nuclear densities over this range, leaving a smooth result. The corresponding charge form factors are shown in Figs. 5 and 6. The vector component is never negligible, but is most important at large q , "pushing out" ${}^3\text{H}$ compared to ${}^3\text{He}$. The heights and positions of the secondary maxima for ${}^3\text{He}$ and ${}^3\text{H}$ are given by

$${}^3\text{He}: F = -1.68 \times 10^{-3}, \text{ at } q_{\text{max}}^2 = 18.7 \text{ fm}^{-2} \quad (8a)$$

and

$${}^3\text{H}: F = -1.93 \times 10^{-3}, \text{ at } q_{\text{max}}^2 = 20.5 \text{ fm}^{-2} \quad (8b)$$

Figure 7 shows the effect of including the Coulomb interaction between the two protons in the 1S_0 partial wave. The effect is small but not entirely negligible and appears to be largely a scale change, pushing charge from the interior to the exterior region in a smooth way. The "hole" in ${}^3\text{He}$ is illustrated by the experimental points with error bars, which were generated by fitting the world data¹⁻⁶ for ${}^3\text{He}$ form factors using a Fourier-Bessel expansion in the manner of Ref. 29. This expansion used 12 Fourier-Bessel coefficients and a cutoff radius of 4 fm, and eliminated the effect of nucleon finite size by the only mechanism possible in the absence of ${}^3\text{H}$ data: by writing

$$\bar{F}_{\text{He}} = (F_s + F_v/2)(G_E^p + G_E^n/2) - \frac{3}{2}F_v G_E^n \quad (9)$$

and ignoring the small $F_v G_E^n$ term. Thus $\bar{F}_{\text{He}}/(G_E^p + G_E^n/2)$ was fit and *no other corrections were made*. The ${}^3\text{He}$ point charge radius obtained in this way is 1.68 fm. Although the hole is graphically obvious and looks like a major feature of the density, it is not. Approximately $\frac{2}{3}$ of one percent of the total charge would completely fill in the depression. The factor of r^2 in the volume element

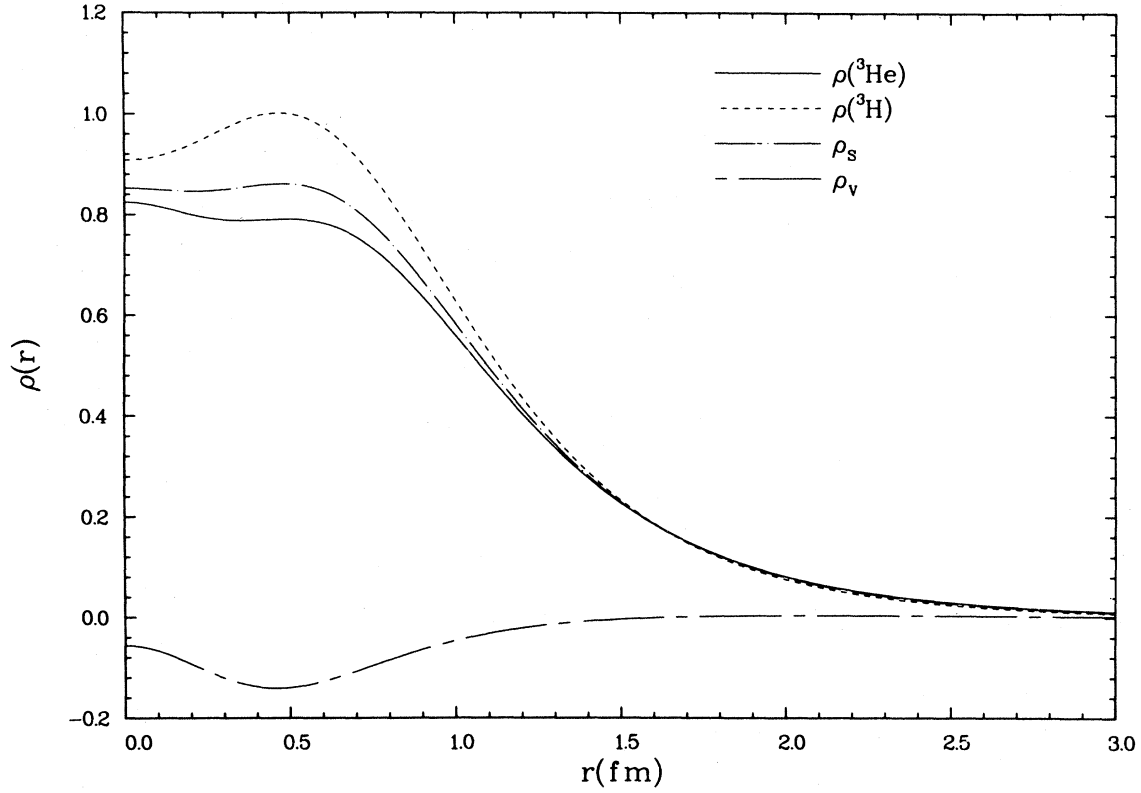


FIG. 3. Various point nucleon charge density components of the trinucleon system calculated using the 5-channel approximation and the Reid soft core potential model.

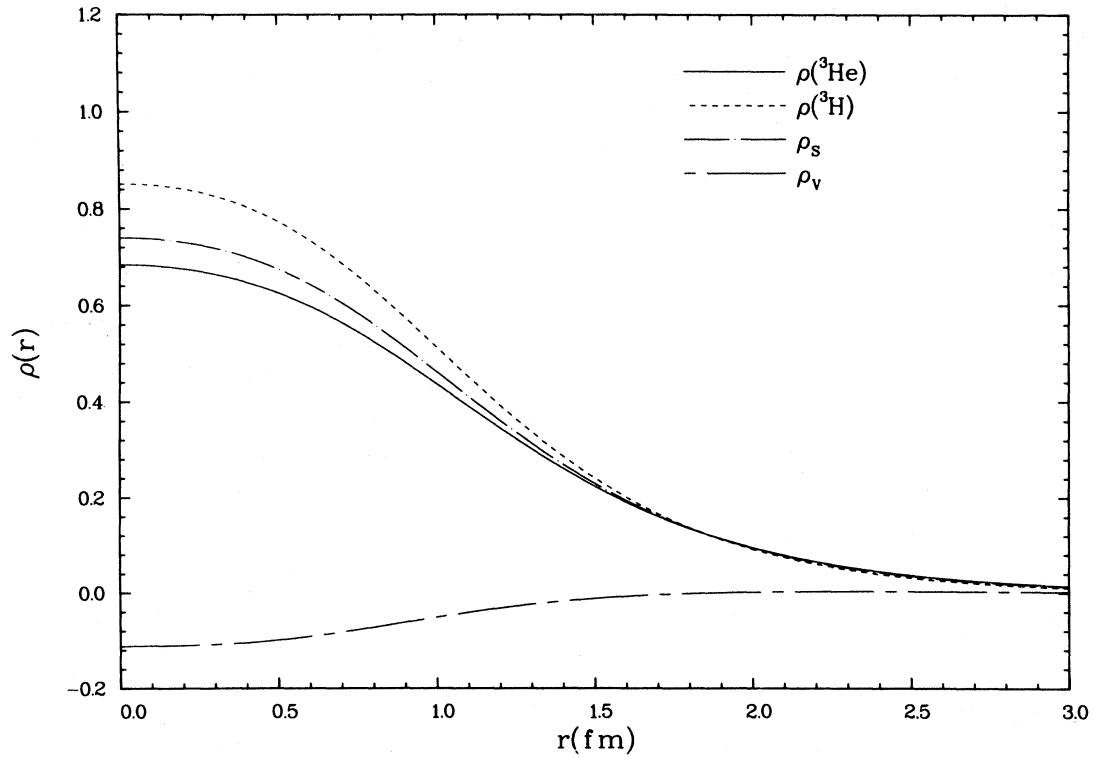


FIG. 4. Various charge density components folded with the nucleon finite size. The model is the same as in Fig. 3.

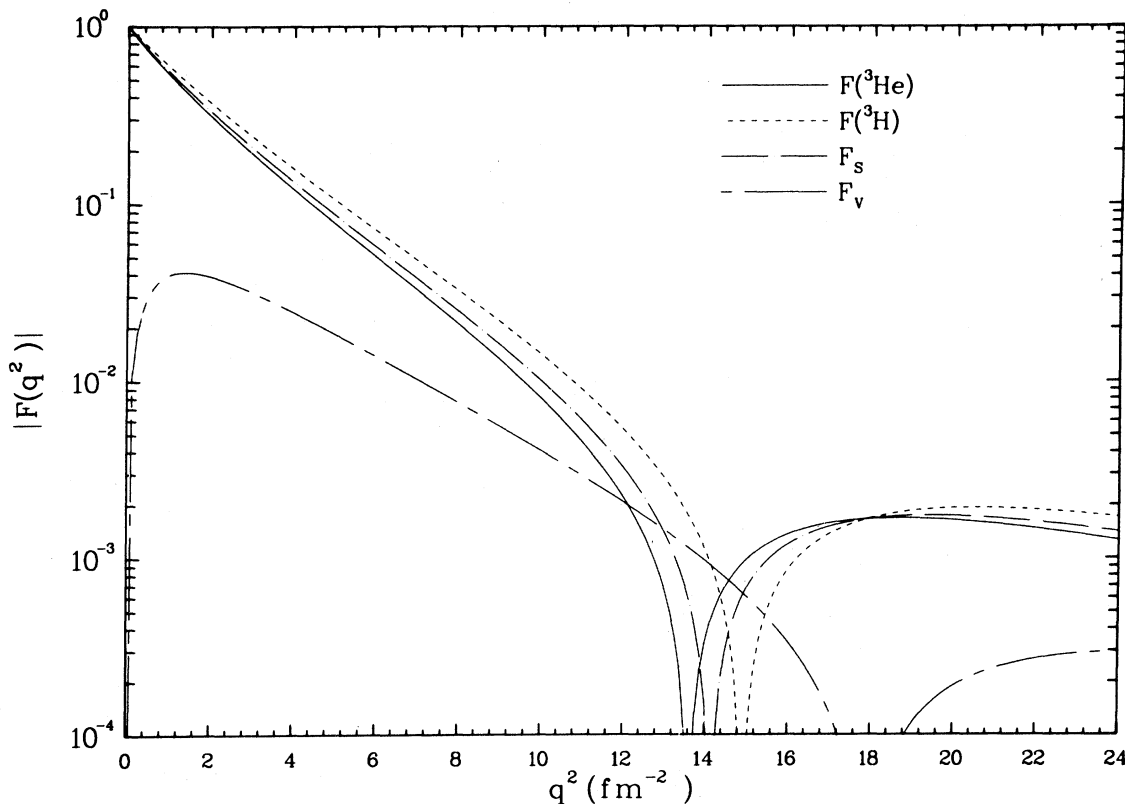


FIG. 5. Various form factors vs momentum transfer q , including the effect of nucleon finite size, for the same model as Fig. 3.

d^3r is responsible for this fact, and for the substantially larger error bars in the interior density than in the surface.²⁹

A total of 10 wave function components³⁰ involving 16 scalar functions is possible in the most general case for the trinucleon ground state. The three 2P states, the solitary 4P state, and the totally space antisymmetric S'' state are tiny and will be ignored. Only the S , S' , and three D wave components are important. In the density itself only certain²⁴ combinations of these components occur:

$$\rho_s = u^2 + (v_1^2 + v_2^2) + (v_3^2 + v_4^2) \quad (10a)$$

and

$$\rho_v = 2uv_1 + (v_3^2 - v_4^2), \quad (10b)$$

where u is the S -state space component, (v_1, v_2) are the S' -state space components, and (v_3, v_4) are the D -state space components, each of which involves three scalar functions. The mixed symmetry functions (v_1, v_2) and (v_3, v_4) satisfy $\int v_1^2 = \int v_2^2$ and $\int v_3^2 = \int v_4^2$, in addition to $\int uv_1 = 0$, so that ρ_v is normalized to zero. The various components of

the theoretical density that lead to the total are illustrated in Fig. 8. The solid line depicts the S and S' components of ρ_s , although the S' contribution is invisible on this scale. The dashed line is the contribution of the SS' overlap in ρ_v , while the contributions of v_3^2 and v_4^2 in ρ_s are separately displayed. It is the structure of v_4^2 which leads to the ripple in ρ_v and to the relatively flat interior density of ρ_s ; the decrease in $\rho(S)$ is compensated by the increase from $\rho(v_4)$. The hole in ^3H near the origin is entirely due to $\rho(v_4)$, since v_3^2 does not contribute to the ^3H density. The RSC3 density differs from that of RSC5 (cf. Figs. 2 and 3) in that ρ_v has a less pronounced kink near the origin, the lack of a hole in ^3H , and pronounced slopes of the densities ρ_s and ρ_{He} near the origin. These are entirely due to the fact that the S -state contribution for RSC3 has a steep downward slope near the origin, and to the slight upward slope of $\rho(SS')$ near the origin.

The lack of a depression in theoretical trinucleon densities is found surprising to many, in view of the strong short-range repulsion in the two-nucleon force which drills deep holes in the wave function. Figure 9 illustrates the Jacobian coordinates conven-

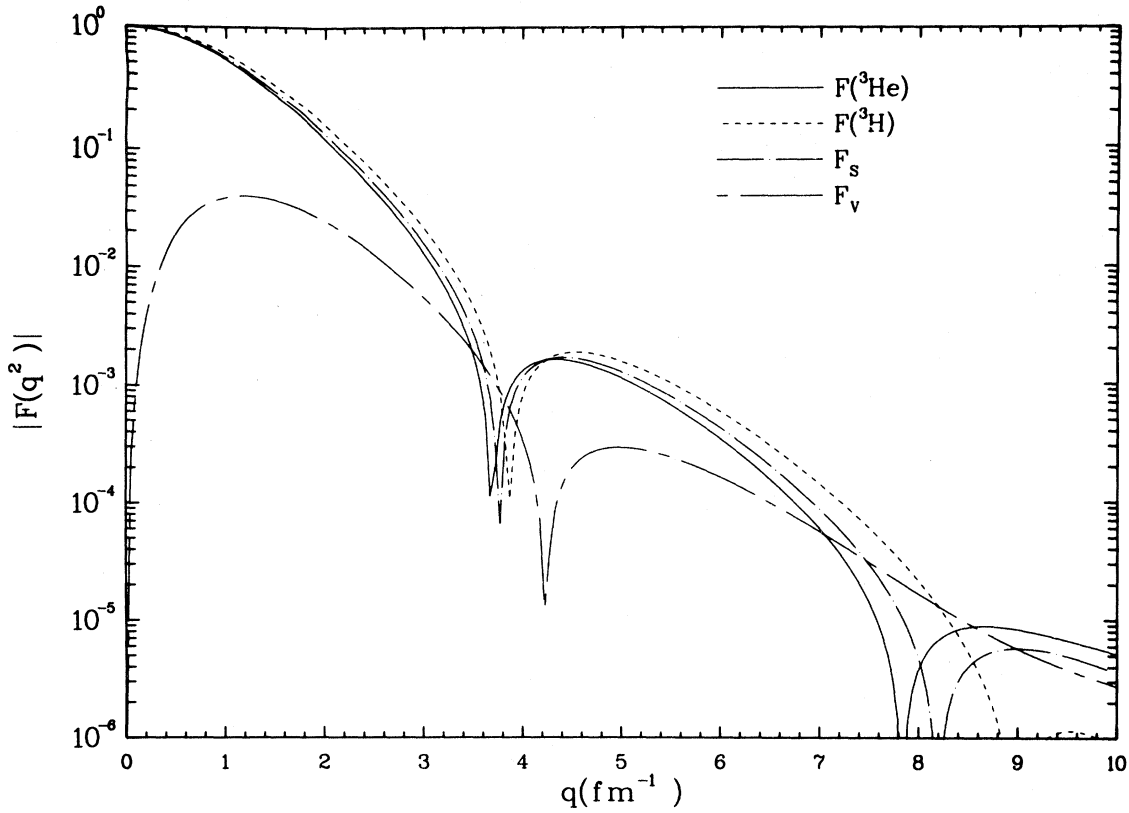


FIG. 6. The same as Fig. 5, but with an expanded range of q , the momentum transfer.

tionally used to label wave functions. Because of the Pauli principle, we can replace the sum over nucleons in Eq. (1) by three times the result for nucleon 1. The δ function then becomes $\delta^3(\vec{r} - \frac{2}{3}\vec{y})$. In order to illustrate how the density is calculated we consider only the principal S -state component $u(x, y, \mu)\phi_a$, where $\mu = \cos\theta$, and ϕ_a is the totally antisymmetric spin-isospin wave function. The density of states is $d^3x d^3y$ and we find

$$\rho(r) = 4\pi\left(\frac{3}{2}\right)^3 \int_0^\infty dx x^2 \int_{-1}^1 d\mu u^2(x, \frac{3}{2}r, \mu); \quad (11a)$$

consequently

$$\rho(0) = 8\pi\left(\frac{3}{2}\right)^3 \int_0^\infty dx x^2 u^2(x, 0, 0). \quad (11b)$$

We have used the fact that when y or r is zero, all three nucleons are in a line and there is no angular dependence (i.e., on μ).

The wave function u for the RSC5 potential model is depicted in Fig. 10 for $\theta = 0^\circ$. In this configuration the nucleons overlap when $y = x/2$, and the strong short range repulsion in the potential is the reason for the deep valley. The wave function is essentially zero when x is small for the same reason.

Nevertheless the $y = 0$ intercept is large, peaking near $x = 2.0$ fm, which is why ρ_s has no central depression for the RSC model. In a more general configuration the existence of strong repulsion makes the wave function small only near $x = 0$. The two D -state combinations v_3^2 and v_4^2 are shown in Figs. 11 and 12. The function v_3^2 has a large $y = 0$ intercept, while v_4^2 is identically zero there, which follows from the definition of the latter function in terms of permutation symmetry [$v_4 \sim \psi_D(\vec{x}_2, \vec{y}_2) - \psi_D(\vec{x}_3, \vec{y}_3)$; $\vec{x}_3 = \vec{x}_2$ and $\vec{y}_3 = -\vec{y}_2$ when $y = 0$; therefore v_4 vanishes since ψ_D is invariant under $\vec{x} \leftrightarrow -\vec{x}$ or $\vec{y} \leftrightarrow -\vec{y}$ for our model problem]. For $y \neq 0$, this condition no longer holds. As y increases from zero, $\rho(v_4)$ increases, accounting for the structure seen in Fig. 8, and ultimately for the hole in ${}^3\text{H}$ seen in Fig. 3.

IV. DISCUSSION AND CONCLUSIONS

Although the hole in ${}^3\text{He}$ has generated considerable theoretical interest because calculations do not reproduce it, it is the least important of the various discrepancies between theory and experiment. The RSC model (without the Coulomb force) generates

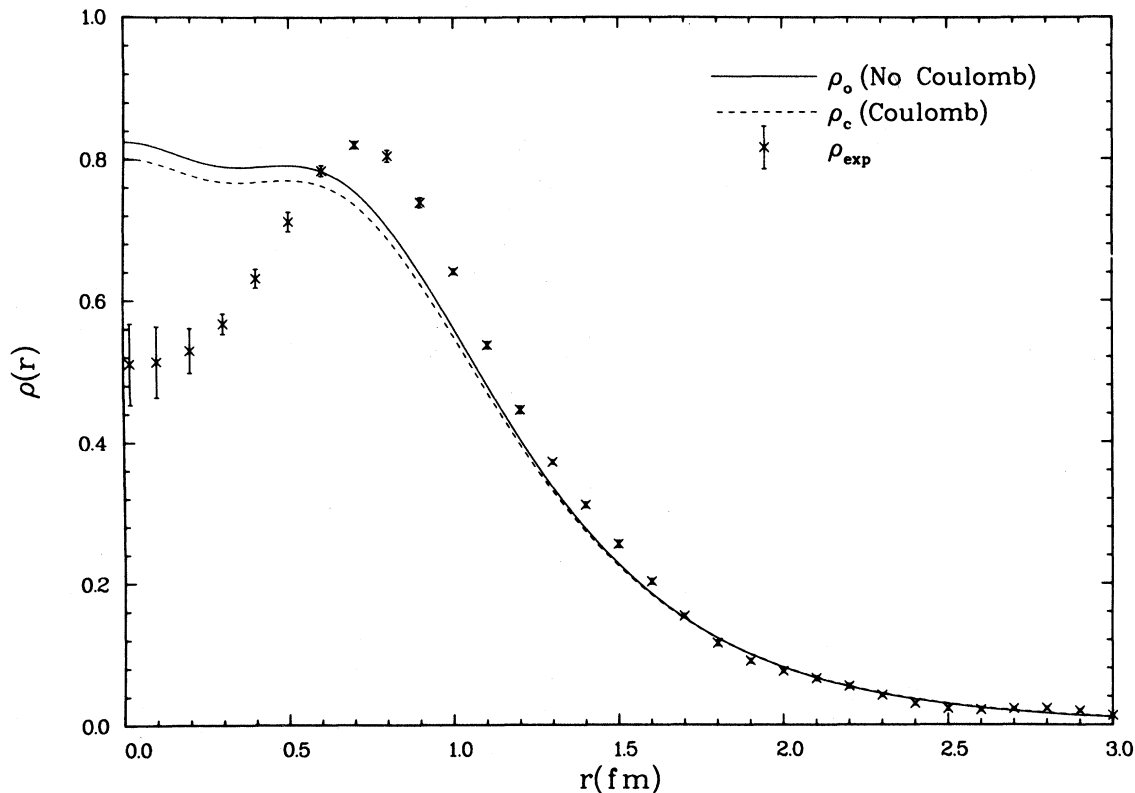


FIG. 7. Point nucleon ${}^3\text{He}$ theoretical charge densities with (ρ_0) and without (ρ_c) the inclusion of the Coulomb interaction, and the corresponding experimental density indicated as data points with error bars.

a total binding energy of approximately 7.3 MeV when the effect of the higher partial waves is included,¹³ compared to the experimental value of 8.54 MeV for tritium. In addition, the calculated (point nucleon) rms charge radius is too large,²²⁻²⁴ 1.70 and 1.93 fm for ${}^3\text{H}$ and ${}^3\text{He}$ (with Coulomb), respectively, compared to 1.56 and 1.68 fm, experimentally. Both deficiencies are consistent and important. More binding presumably will produce a smaller radius.

Several mechanisms have been proposed to deal with these problems.

(1) The current nucleon-nucleon forces are sufficiently inaccurate that better forces will cure most of the problems.

(2) Relativistic effects have not been incorporated in most calculations and these may produce more binding.

(3) Three-body forces cannot be deduced from two-body data and may produce the necessary binding.

(4) In the case of the trinucleon charge form factors, there are meson exchange contributions to the

charge operator which are not included in the impulse approximation, and these can produce changes in the charge density without altering the wave functions.

Although we know of no nucleon-nucleon force models which both fit existing two-body data and do not underbind, it is not possible to rule out possibility (1). Current models which are labeled "realistic" can generate binding energies which differ by several tenths of an MeV. The appellation realistic means *modern* and phenomenologically *adequate*, and in no respect signifies a fundamental understanding of strong interaction dynamics. In view of our ignorance it is hard to assess what physics is missing. The higher partial waves which are lacking in our own and other calculations appear to be relatively unimportant for binding, radius, or central density.³¹ It is tempting to rule out this possibility on the basis of a lack of success to date. However, it appears increasingly likely that there is some element of the tensor force that we currently do not understand. The Mainz experiment³² on photodisintegration of the deuteron with a forward-

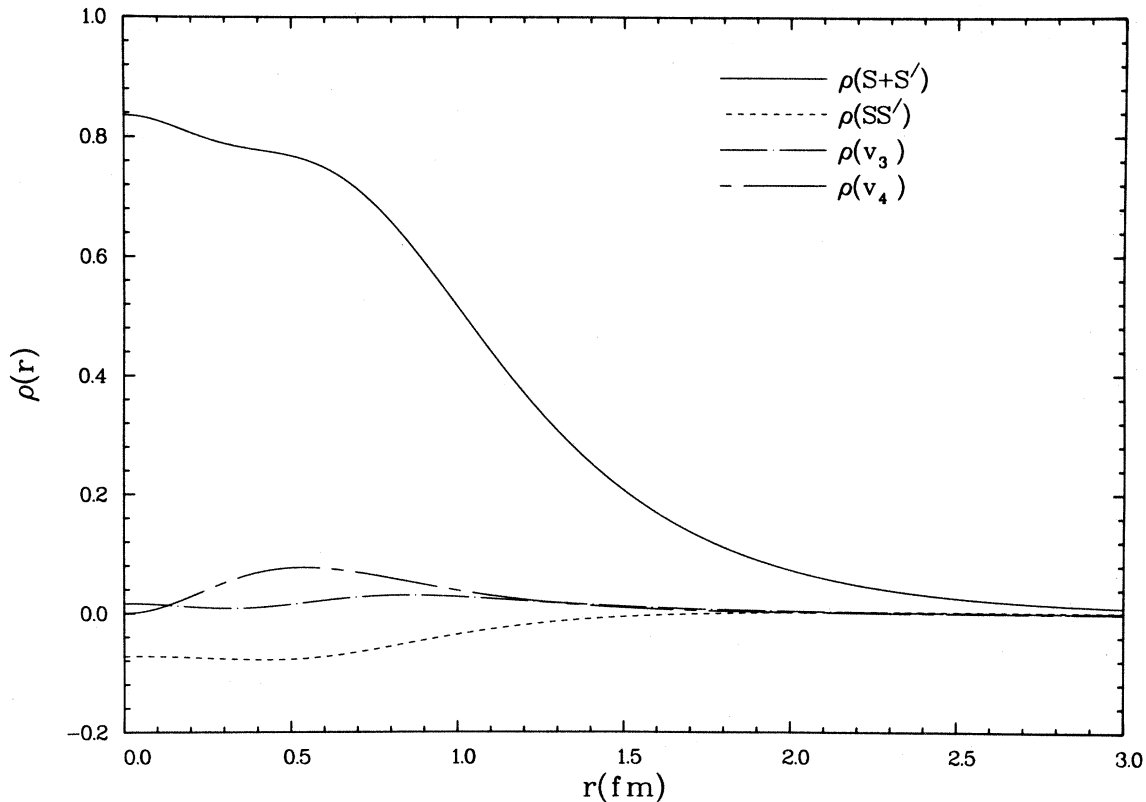


FIG. 8. Contributions to the trinucleon charge densities from the S , S' , and D states. The various entries are described in the text.

going proton is difficult to understand theoretically, and this is extremely sensitive to the tensor force. Theoretical predictions for nuclear matter³³ do not currently agree with “experimental” expectations, and the tensor force plays a very important role there. Note also that the differences between the 3-

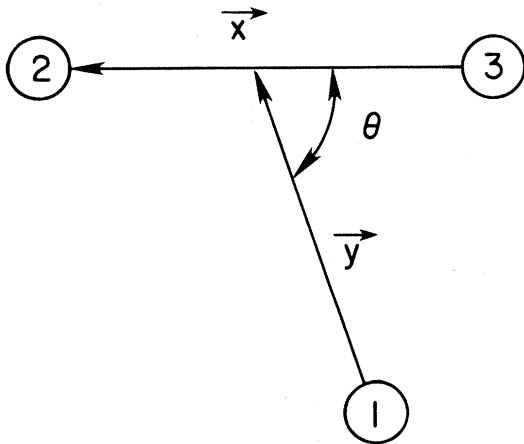


FIG. 9. The Jacobian coordinates \vec{x} , \vec{y} , and θ for the trinucleon system.

and 5-channel Faddeev calculations involve a truncation of the tensor force *only*, and this produces rather large effects in the density. The resolution for these diverse problems may have nothing to do with our problem, but it is impossible to rule out some correlation.

To the best of our knowledge no relativistic calculations have been performed which are *complete* and *unambiguous*.³⁴ Most calculations are incomplete, lacking a comprehensive treatment of the physics. Others have adopted formalisms which may incorporate relativity correctly, but use unrealistic force models, or compare the final results to unrealistic two-body models. Those calculations which have been performed and which are not totally unrealistic largely appear to find a (too) small residual attraction although a small repulsion is not ruled out.⁹

The third possibility appears to us (and others) the most likely to resolve the difficulties we have encountered. Crude estimates³⁵⁻³⁷ of the effect of three-body forces have been performed in the past and much better ones are now being made³⁸; additional attraction is expected and may account for most of the ~ 1 MeV discrepancy. This mechan-

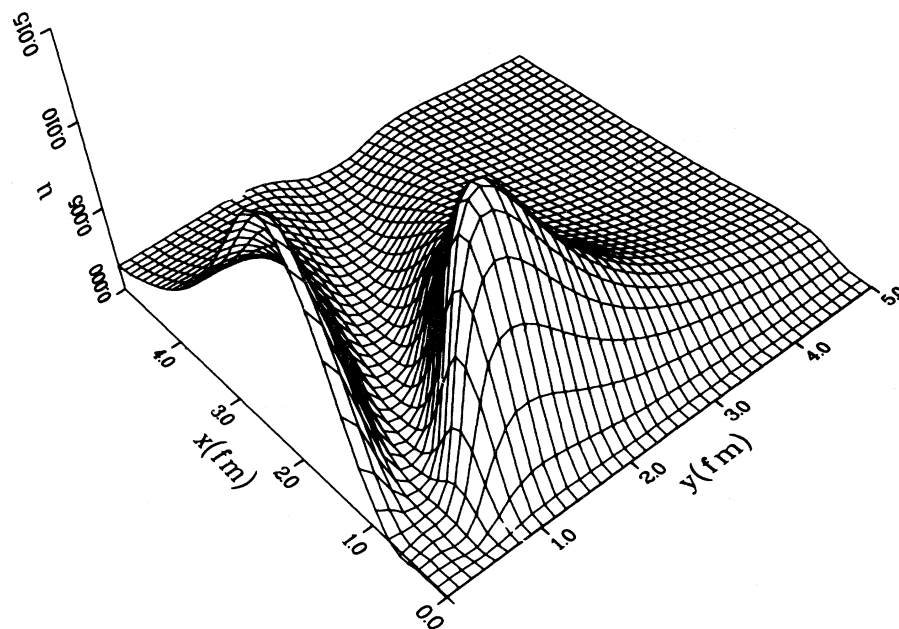


FIG. 10. The principal symmetric S -state function u for the collinear ($\theta = 0^\circ$) configuration plotted as a function of x and y .

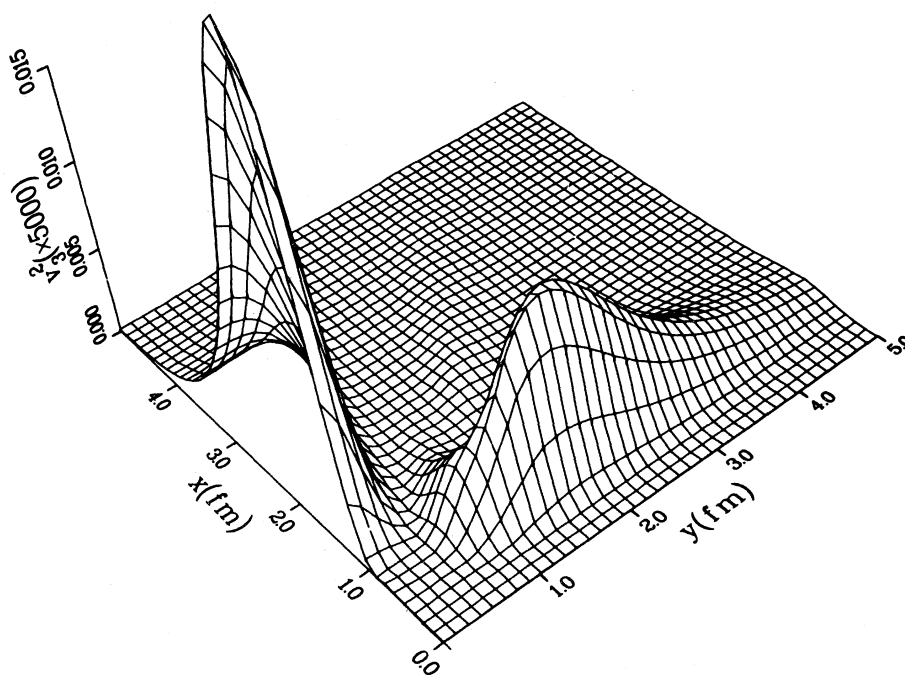


FIG. 11. The D -state component v_3^2 for the collinear configuration ($\theta = 0^\circ$) vs x and y .

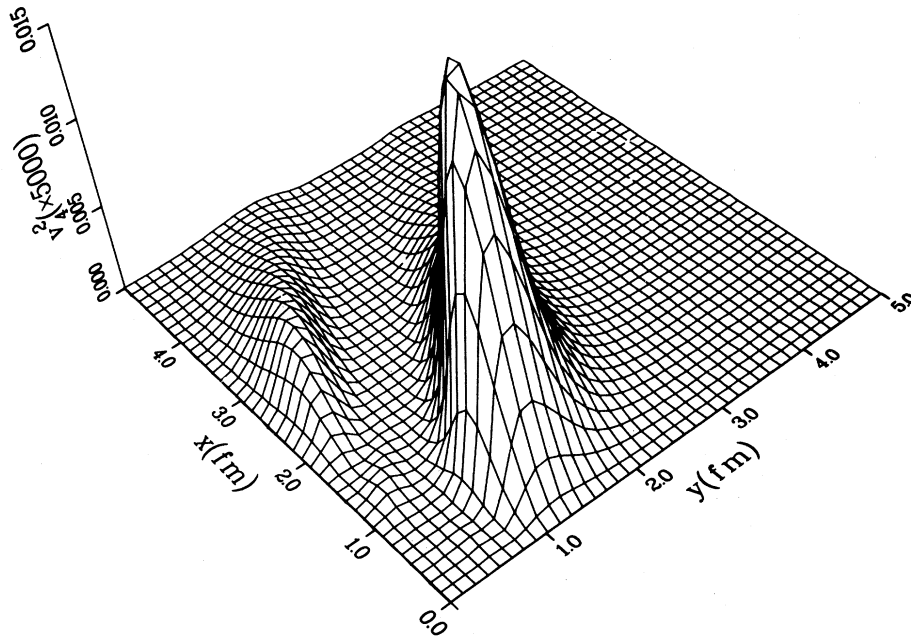


FIG. 12. The D -state component v_4^2 for the collinear configuration ($\theta = 0^\circ$) vs x and y .

ism has the added feature that if the three-body force is repulsive when the nucleons are in a linear configuration (i.e., $r = 0$), the central density will be depleted; it can also be attractive in other angular configurations in order to provide the additional binding. Hopefully, the next two years will do much to clear up the situation with respect to three-body forces. Unfortunately, most of these forces will rely on purely theoretical input, with few (or no) experimental tests of the assumptions used in constructing them.

The meson exchange current problem has been extensively discussed over the past six years.³⁹ To date no internally consistent calculation exists for the three-nucleon system. For the pion exchange currents this would require a *proper* and *consistent* treatment of relativistic corrections to the two- and three-body potentials. Thus all four of the diverse possibilities listed earlier are, in fact, linked together. Other mechanisms, such as the $(\rho\pi\gamma)$ or $(\omega\pi\gamma)$ exchange currents, are not directly linked with the nuclear force, and the same statement applies to certain of the isobar processes. These latter two-body currents have diverse isospin structures,⁴⁰ either $\vec{\tau}(i)\cdot\vec{\tau}(j)$, $[\vec{\tau}(i)\times\vec{\tau}(j)]_3$, or $\tau_3(i)$ for nucleons i and j , and thus will affect ρ_s and ρ_v very differently. In fact, only the $\vec{\tau}(i)\cdot\vec{\tau}(j)$ term contributes to ρ_s ; it is

suppressed in ρ_v by a factor of $-\frac{1}{3}$. The other terms contribute only to ρ_v .

If mesonic corrections to ρ are important it is *absolutely essential to have adequate ^3H charge form factor data*. Although the existence of this data would not by itself resolve all problems, it would greatly facilitate resolution because of the isospin unfolding it would allow. From the low- q data, rms radii can be calculated and one finds $\langle r^2 \rangle_s^{1/2} = 1.65$ and $\langle r^2 \rangle_v^{1/2} = 0.53$ fm compared to 1.86 and 0.75 fm for the RSC5 model. Clearly in this case both scalar and vector components are deficient, being too large by approximately 0.2 fm.

In conclusion, we have investigated the trinucleon ground state charge densities for several potential models and have attempted to correlate the fine structure in these densities with wave function (and isospin) components. The effect of the Coulomb interaction in ^3He was shown to be small but non-negligible. The RSC model predicts a hole in ^3H , unlike ^3He , and this was the result of the D -state components of the wave function. The effect of folding the nucleon charge densities with the point charge densities was to eliminate all visible fine structure in ρ . Finally, we speculated on possible reasons why the experimental and theoretical densities do not agree.

ACKNOWLEDGMENTS

This work was performed under the auspices of the U. S. Department of Energy. We wish to thank

the Q-Division of the Los Alamos National Laboratory (LANL) for generous computational support, and Peter Sauer and Christian Hajduk for discussing their recent results.

-
- ¹H. Collard *et al.*, Phys. Rev. 138, B57(1965).
²Z. M. Szalata *et al.*, Phys. Rev. C 15, 1200 (1977).
³J. S. McCarthy, I. Sick, R. R. Whitney, and M. R. Yearian, Phys. Rev. Lett. 25, 884 (1970).
⁴M. Bernheim *et al.*, Lett. Nuovo Cimerto 5, 431 (1972).
⁵J. S. McCarthy, I. Sick, and R. R. Whitney, Phys. Rev. C 15, 1396 (1977).
⁶R. G. Arnold *et al.*, Phys. Rev. Lett. 40, 1429 (1978).
⁷I. Sick, in *Lecture Notes in Physics* (Springer, Berlin, 1978), Vol. 87, p. 236; *Few Body Systems and Nuclear Forces*, Proceedings of the VIII International Conference on Few Body Systems and Nuclear Forces, Graz, Austria, 1978, edited by H. Zingl, M. Haftel, and H. Zankel (Springer, Berlin, 1978).
⁸R. E. Krepes and J. J. de Swart, Phys. Rev. 162, 1729 (1967).
⁹J. L. Friar, Nucl. Phys. A353, 233 C (1981); Proceedings of the International Conference on the Few-Body Problem, Eugene, Oregon, 1980 (unpublished).
¹⁰R. A. Brandenburg, Y. E. Kim, and A. Tubis, Phys. Rev. C 12, 1368 (1975).
¹¹I. R. Afnan and N. D. Birrell, Phys. Rev. C 16, 823 (1977).
¹²R. A. Brandenburg, P. U. Sauer, and R. Machleidt, Z. Phys. A 280, 93 (1977).
¹³C. Gignoux and A. Laverne, Phys. Rev. Lett. 29, 436 (1972); Nucl. Phys. A203, 597 (1973).
¹⁴T. Sasakawa and T. Sawada, Phys. Rev. C 19, 2035 (1979).
¹⁵M. R. Strayer and P. U. Sauer, Nucl. Phys. A231, 1 (1974).
¹⁶E. Pace, Lett. Nuovo Cimento 26, 615 (1979).
¹⁷M. A. Hennell and L. M. Delves, Nucl. Phys. A246, 490 (1975).
¹⁸C. Ciofi degli Atti, E. Pace, and G. Salmé in *Lecture Notes in Physics* (Springer, Berlin, 1979), Vol. 108, p. 415.
¹⁹J. Lomnitz-Adler and V. R. Pandharipande, Nucl. Phys. A342, 404 (1980).
²⁰J. L. Ballot and M. Fabre de la Ripelle, Ann. Phys. (N.Y.) 127, 62 (1980).
²¹See Fig. 8 of Ref. 7.
²²G. L. Payne, J. L. Friar, B. F. Gibson, and I. R. Afnan, Phys. Rev. C 22, 823 (1980).
²³G. L. Payne, J. L. Friar, and B. F. Gibson, Phys. Rev. C 22, 832 (1980).
²⁴J. L. Friar, E. L. Tomusiak, B. F. Gibson, and G. L. Payne, Phys. Rev. C (in press).
²⁵J. L. Friar, Ann. Phys. (N.Y.) 122, 151 (1979).
²⁶J. L. Friar and B. F. Gibson, Phys. Rev. C 18, 908 (1978).
²⁷G. Höhler *et al.*, Nucl. Phys. B114, 505 (1976).
²⁸R. A. Malfliet and J. A. Tjon, Nucl. Phys. A127, 161 (1969).
²⁹J. L. Friar and J. W. Negele, Adv. Nucl. Phys. 8, 219 (1975).
³⁰G. Derrick and J. M. Blatt, Nucl. Phys. 8, 310 (1958).
³¹Ch. Hajduk and P. U. Sauer, Proceedings of the International Conference on the Few Body Problem, Eugene, Oregon, 1980 (unpublished); and private communication.
³²R. J. Hughes, A. Ziegler, H. Wäffler, and B. Ziegler, Nucl. Phys. A267, 329 (1976).
³³B. Day, Rev. Mod. Phys. 50, 495 (1978).
³⁴Ref. 9 reviews this problem in some detail.
³⁵Ch. Hajduk and P. U. Sauer, in *Lecture Notes in Physics* (Springer, Berlin, 1978), Vol. 82, p. 149.
³⁶E. P. Harper, Y. E. Kim, and A. Tubis, in *Lecture Notes in Physics* (Springer, Berlin, 1978), Vol. 82, p. 153.
³⁷S. N. Yang, Phys. Rev. C 10, 2067 (1974).
³⁸S. Coon and W. Glöckle, private communication; Ch. Hajduk and P. U. Sauer, private communication.
³⁹J. L. Friar, Phys. Rev. C 22, 796 (1980).
⁴⁰J. L. Friar, Ann. Phys. (N.Y.) 104, 380 (1977).